Eur. Phys. J. C (2015) 75:97
DOI 10.1140/epjc/s10052-015-3313-0

THE EUROPEAN PHYSICAL JOURNAL C

Regular Article - Theoretical Physics

Constraints on t-channel leptoquark exchange from LHC contact interaction searches

Assia Bessaa[1,2,3], **Sacha Davidson**[1,2,3,a]

[1] IPNL, CNRS/IN2P3, 4 rue E. Fermi, 69622 Villeurbanne Cedex, France
[2] Université Lyon 1, Villeurbanne, France
[3] Université de Lyon, 69622 Lyon, France

Received: 26 October 2014 / Accepted: 12 February 2015 / Published online: 27 February 2015

Abstract The t-channel exchange of a first generation leptoquark could contribute to the cross section for $q\bar{q} \to e^+e^-$. The leptoquark is off-shell, so this process can be sensitive to leptoquarks beyond the mass reach of pair production searches at the LHC (currently $m_{\rm LQ} > 830$ GeV). We attempt to analytically translate ATLAS bounds on $(\bar{q}\gamma^\mu q)(\bar{e}\gamma_\mu e)$ contact interactions to the various scalar leptoquarks, we but encounter two difficulties: the leptoquark momentum is not negligible, and the leptoquarks do not induce the contact interaction studied by ATLAS, so the interference with the standard model is different. If bounds were quoted on the functional dependence of the cross section on $\hat{s}$, rather than on particular contact interaction models, these difficulties could be circumvented. We use the results of such a "form factor" fit to CMS plots to obtain bounds on the various leptoquarks' quark–lepton coupling of order $\lambda^2 \lesssim (m_{\rm LQ}/3\ {\rm TeV})^2$.

1 Introduction

The LHC has sensitivity to new particles from beyond its kinematic reach, which could materialise as an excess or deficit of events at high energy. Such modifications of the high-energy tail of distributions are commonly parametrised by four-fermion "contact interactions", with coefficient $\pm\frac{4\pi}{\Lambda^2}$. Experimental results are quoted as lower bounds on Λ, for a selection of contact interactions. The question that interests us in this paper, the first of a series, is whether such bounds provide useful constraints on the new physics which could affect the tails of distributions.

Concretely, we will consider the partonic process $q\bar{q} \to e^+e^-$, and assume that the New Physics modifying the high-energy behaviour is a first generation scalar leptoquark (for reviews, see [1–3]), exchanged in the t-channel (see Fig. 1). This process could be sensitive to heavier leptoquarks than could be pair-produced via strong interactions at the LHC (the current bound on pair-produced first generation leptoquarks is $m_{\rm LQ} \gtrsim 830$ GeV [4]). However, this process occurs via the leptoquark–quark–lepton coupling, so it will only be observable for $\mathcal{O}(1)$ couplings.

In this paper, we attempt analytically to estimate bounds on the mass and quark–lepton coupling of the leptoquark, from ATLAS bounds [5] on $(\bar{q}\gamma^\mu P_L q)(\bar{e}\gamma_\mu P_L e)$ contact interactions. Two issues will arise. First, in Sect. 3, we treat the leptoquark exchange as a contact interaction. However, none of the seven possible leptoquarks interfere with the SM in the same way as the ATLAS operator. We attempt to circumvent this problem by assuming the bound comes from the interference term, and making simple approximations to the parton distribution functions (pdfs). The second hurdle is the leptoquark propagator $\sim 1/(m_{\rm LQ}^2 + \hat{s})$, which is taken into account in Sect. 4. As expected, for $m_{\rm LQ} \lesssim 2\sqrt{\hat{s}}$, the propagator reduces the cross section, and therefore weakens the bounds. This effect seems less significant than the consequences of interference, although perverse in the presence of negative interference. Section 5 concludes with a summary of the bounds we obtain on first generation leptoquarks, and a discussion of the difficulties of translating contact interaction bounds to any realistic model without doing a full analysis.

In a second paper [8], an alternate approach to analysing the data in the tails of distributions is studied: if bounds are obtained on the functional form of the cross section, they can be translated in a simple way to many models. This approach was proposed earlier for contact interactions in [6]. After our leptoquark project was completed, CMS presented more restrictive bounds on contact interactions in $q\bar{q} \to e^+e^-$ [7]. The CMS plots were fit to a parametrisation of the functional form of the cross section [8], which avoids both the interference and propagator problems. In a "note-added" to our paper, we combine our results with the fit of [8], to

[a] e-mail: s.davidson@ipnl.in2p3.fr

obtain improved and more reliable bounds on leptoquarks, presented in Table 3.

Combined constraints on leptoquarks, from pair production and single leptoquark exchange in s and t channels, has been studied at HERA (see e.g. [9]). LHC bounds on leptoquarks exchanged in the t-channel were calculated in [10], and for t-channel Z's in [11,12]. Single leptoquark production via t-channel diagrams has also recently been studied in [13].

2 The ATLAS analysis, leptoquarks and kinematics

This section provides a brief overview of the experimental analysis we use [5]; we treat leptoquarks and we present our notation.

ATLAS searched [5] for contact interactions of the form

$$\mathcal{L}_{\rm ATLAS} = \eta\frac{4\pi}{\Lambda^2}\Big[(\bar{d}\gamma^\mu P_L d)(\bar{e}\gamma_\mu P_L e) + (\bar{u}\gamma^\mu P_L u)(\bar{e}\gamma_\mu P_L e)\Big] \quad (1)$$

where $\eta = +/-1$ corresponds to destructive/constructive interference with Z/γ exchange. The 95 % confidence level (CL) bounds obtained with 5 fb^{-1} of data at $\sqrt{s} = 7$ TeV are

$$\Lambda_{\rm con} \gtrsim 11.75\,{\rm TeV}, \quad \Lambda_{\rm des} \gtrsim 9.3\,{\rm TeV}. \quad (2)$$

The analysis presents the number of events expected and observed as a function of the invariant mass-squared of the e^+e^- pair

$$M^2_{e^+e^-} = \hat{s} = x_1 x_2 s \quad (3)$$

in bins of width given in the left column of Table 1. The background calculated by ATLAS includes $q\bar{q} \to Z/\gamma \to e^+e^-$, as well as other SM processes such as $t\bar{t}$ production and dibosons.

We consider scalar leptoquarks, with renormalisable B and L conserving interactions, which generate an interaction between first generation quarks and electrons. In the notation of Buchmuller et al. [14], the leptoquark interactions with quarks and leptons can be added to the SM Lagrangian, thus:

$$\begin{aligned}\mathcal{L}_{\rm LQ} = {} & S_0(\lambda_{LS_0}\bar{\ell}i\tau_2 q^c + \lambda_{RS_0}\bar{e}u^c) + \tilde{S}_0\tilde{\lambda}_{R\tilde{S}_0}\bar{e}d^c \\ & + S_2(\lambda_{LS_2}\bar{\ell}u + \lambda_{RS_2}\bar{e}q[i\tau_2]) + \tilde{S}_2\tilde{\lambda}_{L\tilde{S}_2}\bar{\ell}d \\ & + \vec{S}_1\lambda_{LS_1}\bar{\ell}i\tau_2\vec{\tau}q^c\cdot + h.c. \end{aligned} \quad (4)$$

where τ_2 is a Pauli matrix, so $i\tau_2$ provides the antisymmetric SU(2) contraction.

These leptoquarks can contribute to $q\bar{q} \to e^+e^-$ (where $q \in \{u, d\}$) via t-channel exchange. The diagrams and interfering SM processes are given in Fig. 1. It is convenient to write the matrix element $\mathcal{M}(\bar{q}q_X \to e^+e^-_Y)$ as a spinor contraction $\mathcal{T}_{XY}$ multiplied by a propagator $\mathcal{P}_{q_X e_Y}$. For instance, for S_o with coupling λ_R, the spinor contraction after a Fiertz transformation can be written $\mathcal{T}_{RR} = (\bar{u}\gamma^\mu P_R u)(\bar{e}\gamma_\mu P_R e)$. For $XX \in \{LL, RR\}$ or $XY \in \{LR, RL\}$

$$\overline{|\mathcal{T}_{XX}|^2} = \frac{\hat{u}^2}{3}, \quad \overline{|\mathcal{T}_{XY}|^2} = \frac{\hat{t}^2}{3}, \quad (\hat{u} = -2p_2\cdot k_1, \hat{t} = -2p_1\cdot k_1) \quad (5)$$

where the bar indicates an average over incident colour and spin, the momenta are as in Fig. 1 and

$$\frac{{\rm d}\hat{\sigma}}{{\rm d}\hat{t}} = \frac{\overline{|\mathcal{M}|^2}}{16\pi\hat{s}^2} \text{ with } \overline{|\mathcal{M}|^2} = \overline{|\mathcal{T}|^2}|\mathcal{P}|^2. \quad (6)$$

The contact interaction analysis of ATLAS is at $\hat{s} > (400\ {\rm GeV})^2$, so we neglect m_Z and propagate the massless B and W^0. Then the propagators of Fig. 1 give

$$i\mathcal{P}_{q_X e_Y} = \Big(Y_{e_Y}Y_{q_X}g'^2 + T_{e_Y}T_{q_X}g^2\Big)\frac{1}{\hat{s}} - (-1)^{F/2}\frac{\lambda^2}{2(m^2_{\rm LQ} - \hat{\tau})}(\times 2) \quad (7)$$

where F is the fermion number of the leptoquark, which is 2 for doublet leptoquarks and 0 otherwise, $\hat{\tau} = \hat{t}$ for $F = 0$ leptoquarks and $\hat{u}$ for $F = 2$, and the $(\times 2)$ applies only in the case of triplet leptoquark exchange coupled to d quarks. Recall that the hypercharge and SU(2) quantum numbers of the SM fermions are

$$Y_{e_L} = -\frac{1}{2}, Y_{e_R} = -1, Y_{q_L} = \frac{1}{6}, Y_{u_R} = \frac{2}{3}, Y_{d_R} = -\frac{1}{3},$$
$$T_{e_L} = T_{d_L} = -\frac{1}{2}T_{u_L} = \frac{1}{2}.$$

For each leptoquark, the Fierz-rearranged $\bar{q}qe^+e^-$ vertices, with the appropriate propagators representing Z/γ and leptoquark exchange, are given in column two of Table 2. To obtain the contact interaction mediated by a leptoquark, $\tau \to 0$ in this table and the SM part of the propagator should be dropped. In most cases, the coefficient of the contact interaction is $\lambda^2/(2m^2_{\rm LQ})$.

Table 1 In the first column, bins of dilepton mass $M_{e^+e^-}$ (where $M^2_{e^+e^-} = (p_e + p_{\bar{e}})^2$). The following columns are from the ATLAS paper [5]: the expected number of events due to the SM, due to the SM plus a contact interaction with $\Lambda = 12$ TeV and constructive interference with the SM, and finally the data

Bin (GeV)	Z/γ + other SM	All SM + $\Lambda_{\rm cons} = 12$ TeV	Data
400–550	$203 + 73 \pm 25$	293 ± 27	270
550–800	$62 + 20 \pm 9$	96 ± 9	88
800–1200	$12.1 + 3.2 \pm 2$	23.6 ± 2.3	17
1200–1800	$1.38 + 0.36 \pm 0.33$	5.1 ± 0.5	3
1800+	$0.085 + 0.035 \pm 0.04$	0.87 ± 0.14	0

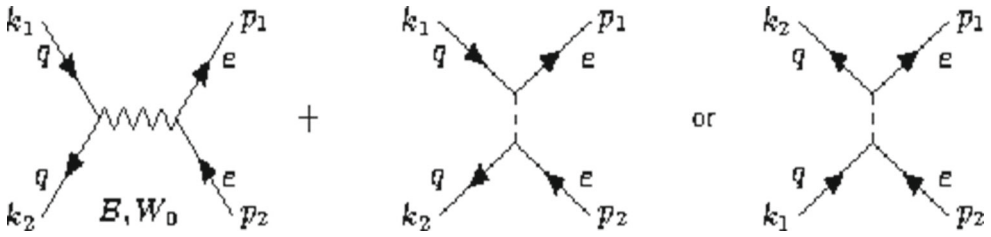

Fig. 1 Possible SM and leptoquark diagrams for $q\bar{q} \to e^+e^-$, in the limit of neglecting m_Z. Only one leptoquark diagram will be present at a time; the central diagram is for fermion number $F = 0$ leptoquarks [the SU(2) doublets], the last diagram for fermion number $F = 2$ leptoquarks [the SU(2) triplets and singlets]. Momenta k enter the graph and momenta p leave

Notice that the angular distribution of the leptons is relatively homogeneous, and does not discriminate the leptoquark from SM contributions. This is because the SM is s-channel, and the lower bounds on leptoquark masses prevent a significant growth of the leptoquark propagator at small $\hat{t}$. This is different from contact interaction searches in $qq \to qq$, where t-channel gluon exchange causes the SM contribution to diverge along the beam-pipe.

ATLAS bins its data in $\hat{s} = M^2_{e^+e^-}$ (see Eq. 3), so it is convenient to express the total cross section for $pp \to e^+e^-$ as

$$\sigma = \sum_{q=u,d} \frac{1}{s} \int \mathrm{d}\hat{s}\, \mathrm{d}\eta^+\, \mathrm{d}\hat{t}\, f_q(x_1) f_{\bar{q}}(x_2) \left[\frac{\mathrm{d}\hat{\sigma}_{Z/\gamma}(\hat{t})}{\mathrm{d}\hat{t}} + \frac{\mathrm{d}\hat{\sigma}_{\mathrm{NP}}(\hat{t})}{\mathrm{d}\hat{t}} + \frac{\mathrm{d}\hat{\sigma}_{Z/\gamma}(\hat{t} \leftrightarrow \hat{u})}{\mathrm{d}\hat{t}} + \frac{\mathrm{d}\hat{\sigma}_{\mathrm{NP}}(\hat{t} \leftrightarrow \hat{u})}{\mathrm{d}\hat{t}} \right] \tag{8}$$

where f_q is the parton distribution function (pdf) for the quark q in the proton, $x_1 = \frac{M_{e^+e^-}}{\sqrt{s}} e^{\eta_+}$ and $x_2 = \frac{M_{e^+e^-}}{\sqrt{s}} e^{-\eta_+}$ are the fraction of the proton's momentum carried by the parton, the cross section is separated into the gauge boson mediated part plus a New Physics part, and the $\hat{t} \leftrightarrow \hat{u}$ terms account for the valence quarks possibility to be in either incident proton. The integration limits on $\eta_+ = (\eta_e + \eta_{\bar{e}})/2$ and $\hat{t}$ should be determined from the experimental cuts on the rapidities η_{e^+}, η_{e^-} of the e^+e^-, however, for simplicity, we integrate over the whole phase space. The resulting error is negligeable, because at fixed $\hat{s}$, $\frac{\mathrm{d}\hat{\sigma}}{\mathrm{d}\hat{t}}$ varies by factors of a few over all angles, so neglecting a small cone makes little difference to the result of the angular integration.

3 Leptoquark exchange as a contact interaction

In this section, we approximate leptoquark exchange as a contact interaction, and try to constrain the leptoquark-mediated contact interactions from the ATLAS analysis. The challenge will be to deal with the different flavours and chiralities of the leptoquark-induced operators, which will affect the number of New Physics events, and the distribution in $M^2_{e^+e^-}$. To see this, the total cross section of Eq. (8) can be written

$$\frac{\mathrm{d}\sigma(pp \to e^+e^-)}{\mathrm{d}\hat{s}} = C(\hat{s}) \frac{\hat{s}}{s} \left(\frac{11 g^4}{96 \hat{s}^2} + \epsilon_{\mathrm{int}} \frac{g^2}{\hat{s}} \frac{\lambda^2}{2m^2_{\mathrm{LQ}}} + \epsilon_{\mathrm{NP}} \frac{\lambda^4}{4m^4_{\mathrm{LQ}}} \right), \tag{9}$$

where the NP part is divided into the cases of interference with the SM and of interference with itself. $C(\hat{s})$ is dimensionless, fixed by the electroweak interactions of the quarks and electrons, and includes an integral over the pdfs. The ϵs are also dimensionless and satisfy $-\sqrt{11/24} \leq \epsilon_{\mathrm{int}}/\sqrt{\epsilon_{\mathrm{NP}}} \leq \sqrt{11/24}$. The magnitude of ϵ_{NP} will depend on which flavours of quark couple to a given leptoquark, and the magnitude and sign of ϵ_{int} will depend on the flavour and chirality of the participating fermions, because these control the interference with the γ/Z.

To analytically compare the ϵs induced by leptoquarks, to those arising from the ATLAS contact interaction, we assume simplistic relations among the parton distribution functions (pdfs) in the proton, such that

$$f_u(x) = 2 f_d(x), \quad f_{\bar{u}}(x) = f_{\bar{d}}(x) \tag{10}$$

which will allow one to estimate ϵ_{int} and ϵ_{NP} from the partonic matrix elements (given in the second column of Table 2).

To make such estimates, we first schematically write the partonic Z/γ-exchange cross section, multiplied by pdfs, as

$$\begin{aligned} \text{pdfs} \times \frac{\mathrm{d}\hat{\sigma}}{\mathrm{d}\hat{t}} &= \frac{\hat{t}^2}{48\pi \hat{s}^4} \\ &\times \Big[g^4 T_e^2 (f_u f_{\bar{u}} T_u^2 + f_d f_{\bar{d}} T_d^2) + 2 g^2 g'^2 T_e Y_{e_L} [T_u Y_{u_L} f_u f_{\bar{u}} \\ &+ T_d Y_{d_L} f_d f_{\bar{d}}] + g'^4 (Y^2_{e_L} + Y^2_{e_R}) (f_u f_{\bar{u}} [Y^2_{u_L} + Y^2_{u_R}] \\ &+ f_d f_{\bar{d}} [Y^2_{d_L} + Y^2_{d_R}]) \Big], \end{aligned}$$

where inside the square brackets is the pdf-weighted "propagator" $|\mathcal{P}|^2$ of Eq. (7), multiplied by $\hat{s}^2$. With the approximation $s^2_W = 1/4$ and Eq. (10)

$$\begin{aligned} \frac{\mathrm{d}\sigma_{Z/\gamma}}{\mathrm{d}\hat{s}} &\simeq \frac{11}{96} \frac{g^4}{\hat{s}} \frac{1}{72\pi s} \int \mathrm{d}\eta_+ (f_u f_{\bar{u}} + f_d f_{\bar{d}}) \\ &\Rightarrow C(\hat{s}) = \frac{1}{72\pi} \int \mathrm{d}\eta_+ (f_u f_{\bar{u}} + f_d f_{\bar{d}}) \end{aligned} \tag{11}$$

Table 2 Fierz-transformed two-electron–two quark matrix elements induced by the leptoquark, γ and Z exchange diagrams of Fig. 1, in the limit $m_Z \to 0$ (possible quark-neutrino interactions are not included). $\hat{\tau}$ can be $\hat{t}$ or $\hat{u}$. The third and fourth columns estimate the coefficients in Eq. (9), using the approximation of Eq. (10). The second last column is the bound on λ^2, for $m_{\rm LQ} = 2$ TeV, assuming the ATLAS limits on contact interactions can be translated to leptoquarks using Eq. (13) (or Eq. (14) for the limits in parentheses). The last column is an estimate of the confidence level (see Eq. 16) of that bound, obtained with the cross section of Eq. (9)

Interaction	Fierz-transformed $\mathcal{M}$	$\epsilon_{\rm int}$	$\epsilon_{\rm NP}$	$\lambda^2\left(\frac{(2\text{TeV})^2}{m_{\rm LQ}^2}\right) <$	CL
ATLAS	$+,-\Big[(\bar{u}\gamma^\mu P_L u)(\bar{e}\gamma_\mu P_L e)\left(\frac{\lvert\lambda\rvert^2}{2m^2}-\frac{1}{4}\frac{g^2}{\hat{s}}\right)$ $+(\bar{d}\gamma^\mu P_L d)(\bar{e}\gamma_\mu P_L e)\left(\frac{\lvert\lambda\rvert^2}{2m^2}+\frac{1}{4}\frac{g^2}{\hat{s}}\right)\Big]$	$-\frac{1}{6},+\frac{1}{6}$	1	1.1, 0.73	67 %, 84 %
$(\lambda_{LS_o}\overline{q^c}i\sigma_2\ell+\lambda_{RS_o}\overline{u^c}e)S_o^\dagger$	$(\bar{u}\gamma^\mu P_R u)(\bar{e}\gamma_\mu P_R e)\left(\frac{\lvert\lambda_R\rvert^2}{2(m_o^2-\hat{\tau})}-\frac{2}{3}\frac{g'^2}{\hat{s}}\right)$	$-\frac{8}{27}$	$\frac{2}{3}$	0.65	82 %
	$(\bar{u}\gamma^\mu P_L u)(\bar{e}\gamma_\mu P_L e)\left(\frac{\lvert\lambda_L\rvert^2}{2(m_o^2-\hat{\tau})}-\frac{1}{4}\frac{g^2}{\hat{s}}\right)$	$-\frac{1}{3}$	$\frac{2}{3}$	0.58	85 %
$\lambda_{R\tilde{S}_o}\overline{d^c}e\tilde{S}_o^\dagger$	$(\bar{d}\gamma^\mu P_R d)(\bar{e}\gamma_\mu P_R e)\left(\frac{\lvert\lambda_R\rvert^2}{2(\tilde{m}_o^2-\hat{\tau})}+\frac{1}{3}\frac{g'^2}{\hat{s}}\right)$	$\frac{2}{27}$	$\frac{1}{3}$	1.6	89 %
$(\lambda_L\bar{u}\ell+\lambda_R\bar{q}i\sigma_2 e)S_2^\dagger$	$(\bar{u}\gamma^\mu P_R u)(\bar{e}\gamma_\mu P_L e)\left(-\frac{\lvert\lambda_L\rvert^2}{2(m_2^2-\hat{\tau})}-\frac{1}{3}\frac{g'^2}{\hat{s}}\right)$	$\frac{4}{27}$	$\frac{2}{3}$	0.9	84 %
	$(\bar{u}\gamma^\mu P_L u)(\bar{e}\gamma_\mu P_R e)\left(-\frac{\lvert\lambda_R\rvert^2}{2(m_2^2-\hat{\tau})}-\frac{1}{6}\frac{g'^2}{\hat{s}}\right)$				
	$+(\bar{d}\gamma^\mu P_L d)(\bar{e}\gamma_\mu P_R e)\left(-\frac{\lvert\lambda_R\rvert^2}{2(m_2^2-\hat{\tau})}-\frac{1}{6}\frac{g'^2}{\hat{s}}\right)$	$\frac{1}{9}$	1	1.1	92 %
$\lambda_{L\tilde{S}_2}\bar{d}\ell\tilde{S}_2^\dagger$	$(\bar{d}\gamma^\mu P_R d)(\bar{e}\gamma_\mu P_L e)\left(-\frac{\lvert\lambda_L\rvert^2}{2(\tilde{m}_2^2-\hat{\tau})}+\frac{1}{6}\frac{g'^2}{\hat{s}}\right)$	$-\frac{1}{27}$	$\frac{1}{3}$	(1.64)	(86 %)
$\lambda_{LS_1}\overline{q^c}i\sigma_2\vec{\sigma}\ell\cdot\vec{S}_1{}^\dagger$	$(\bar{u}\gamma^\mu P_L u)(\bar{e}\gamma_\mu P_L e)\left(\frac{\lvert\lambda_L\rvert^2}{2(m_1^2-\hat{\tau})}-\frac{1}{4}\frac{g^2}{\hat{s}}\right)$				
	$+(\bar{d}\gamma^\mu P_L d)(\bar{e}\gamma_\mu P_L e)\left(\frac{\lvert\lambda_L\rvert^2}{(m_1^2-\hat{\tau})}+\frac{1}{4}\frac{g^2}{\hat{s}}\right)$	$\simeq 0$	4/3	(0.80)	(86 %)

where the pdf integral over η_+ is a constant that we do not need to know. (We also neglected experimental cuts in integrating over $\hat{t}$, which is hopefully an acceptable approximation because the $\hat{t}$ dependence of $|\mathcal{T}|^2$ is common to the SM and NP, and there is no $\hat{t}$ dependence of the propagators in the contact approximation.)

The ATLAS analysis [5] follows Pythia [15] in summing over u and d flavours, and it is restricted to doublet ("left-handed") quarks. Using again the approximation (10), and identifying $4\pi/\Lambda^2 = \lambda^2/2m^2$, the cross section in the presence of the ATLAS contact interaction, with constructive interference with the SM, can be approximated as

$$\frac{\mathrm{d}\sigma_{CI}}{\mathrm{d}\hat{s}} \simeq \frac{\mathrm{d}\sigma_{Z/\gamma}}{\mathrm{d}\hat{s}} + \left(\frac{1}{6}\frac{g^2}{\hat{s}}\frac{\lambda^2}{2m^2}+\frac{\lambda^4}{4m^4}\right)\frac{\hat{s}}{72\pi s} \times \int \mathrm{d}\eta_+ (f_u f_{\bar{u}} + f_d f_{\bar{d}}) \tag{12}$$

so $\epsilon_{\rm int} = \pm 1/6$ and $\epsilon_{NP} = 1$ for the ATLAS contact interaction.

The contact interactions induced by the various leptoquarks differ from the one studied by ATLAS, as can be seen from the second column of Table 2. The values of $\epsilon_{\rm int}$ and $\epsilon_{\rm NP}$ can be estimated, as above, and are given in Table 2. One sees that the leptoquarks with constructive interference (positive $\epsilon_{\rm int}$) have a smaller $\epsilon_{\rm int}/\sqrt{\epsilon_{\rm NP}}$ ratio than the ATLAS operator. So one could hope to constrain these leptoquarks by simply rescaling the ATLAS bound. We conservatively rescale the bound as

$$\epsilon_{\rm int}\frac{4\pi}{\Lambda^2}\Big|_{\rm ATLAS} \geq \epsilon_{\rm int}^{\rm LQ}\frac{\lambda^2}{2m_{\rm LQ}^2} \tag{13}$$

where $\Lambda_{\rm cons} = 11.7$ TeV and $\epsilon_{\rm int} = 1/6$ on the left side. For the leptoquark S_2 with coupling λ_L, this excludes above the red diagonal line of the left Fig. 2.

Analytic estimates suggest that Eq. (13) is conservative: if the bound arises from the interference term, then one expects $\epsilon_{\rm int}^{\rm ATLAS}\frac{4\pi}{\Lambda^2} \simeq \epsilon_{\rm int}^{\rm LQ}\frac{\lambda^2}{2m_{\rm LQ}^2}$. However, if the bound came from the $|\text{NP}|^2$ term, then one might expect $\sqrt{\epsilon_{\rm NP}^{\rm ATLAS}}\frac{4\pi}{\Lambda^2} \simeq \sqrt{\epsilon_{\rm NP}^{\rm LQ}}\frac{\lambda^2}{2m_{\rm LQ}^2}$, which would give a stronger bound on the leptoquark couplings. For the ATLAS contact interaction, and leptoquark-induced contact interactions with $\epsilon_{\rm int}/\sqrt{\epsilon_{\rm NP}} \simeq 1/6$, the NP^2 term becomes larger than the interferences at $\sqrt{\hat{s}} \gtrsim 900$ GeV, so it dominates the last bin with data (= 1200 TeV $< \sqrt{\hat{s}} <$ 1800 TeV).

For leptoquarks that have destructive interference with the SM, the ratio $\epsilon_{\rm int}/\sqrt{\epsilon_{\rm NP}}$ departs significantly from the ratio

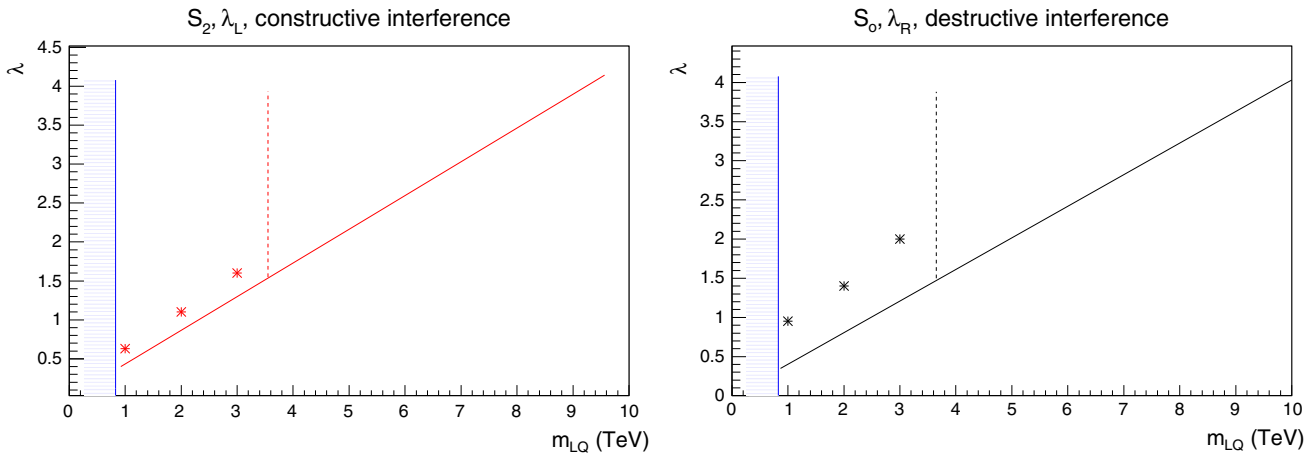

Fig. 2 The parameter space above the diagonal line is excluded by the contact interaction bound given in Table 2. *Left plot* for S_2 with coupling λ_L, *right plot* for S_o with coupling λ_R. The *blue region* to the *left* with *horizontal hashes* is excluded by CMS searches [4] for pairs of first generation leptoquarks. The cross sections for the contact interaction and with the leptoquark propagator agree within 20 % to the *right* of the *dashed line*; if the leptoquark propagator is taken into account, only the region *above* the *stars* is excluded (see Sect. 4)

of the ATLAS operator. Nonetheless we again take the translation rule of Eq. (13) with $\Lambda_{\rm des} \geq 9.3$ TeV. In the second last column of Fig. 2, Eq. (13) is used to translate the ATLAS bound to most of the singlet and doublet leptoquarks. On the right in Fig. 2 the exclusion is plotted for S_o with coupling λ_R. The next subsection contains some simple statistics to estimate the credibility of Eq. (13).

In the case of the triplet leptoquark S_1 and the doublet $\tilde{S}_2$, the interference almost vanishes, so a bound was estimated from the $|\mathrm{NP}|^2$ term, thus:

$$\frac{4\pi}{\Lambda^2}\Big|_{\rm ATLAS} \geq \sqrt{\epsilon_{\rm NP}}\frac{\lambda^2}{2m_{\rm LQ}^2}, \tag{14}$$

where $1/\Lambda^2$ on the left side is the average of the ATLAS constructive and destructive bounds $\frac{1}{2}\left(\frac{1}{11.7^2}+\frac{1}{9.3^2}\right)$. The bounds estimated from Eq. (14) are given in parentheses in Table 2.

3.1 Comparing partonic cross sections to ATLAS data

None of the leptoquarks induce the contact interaction constrained by ATLAS, so it is not clear how to translate the ATLAS bound to leptoquarks. In particular, the shape in $\hat{s}$ of the differential cross section, Eq. (9), will depend on the different values of the ϵs. This will change the number of New Physics events in the ATLAS bins, and it affect the overall deviation from the SM. The aim of this subsection is to confirm that Eq. (13) is conservative, using simple statistics and partonic cross sections.

We focus on the last three ATLAS bins in $\hat{s}$ (see Table 1) and assume that the pdfs are decreasing fast enough with increasing $\hat{s}$. Thus, in each bin b, the number of signal NP events plus background SM events can be estimated as

$$(r_b^{\rm NP}-1)n(Z/\gamma)+n(\mathrm{SM}),\quad r_b^{\rm NP}\equiv\frac{\hat{\sigma}_{Z/\gamma+\mathrm{NP}}(\hat{s})}{\hat{\sigma}_{Z/\gamma}(\hat{s})}. \tag{15}$$

Here $r_b^{\rm NP}$ is the ratio of the $Z/\gamma+\mathrm{NP}$ cross section of Eq. (9) to the Z/γ cross section (this neglects experimental acceptances), taken at the left side of each $\hat{s}$ bin, calculated for $m_{\rm LQ}=2$ TeV with the value of λ^2 given in the second last column of Table 2. Also we use the correct $\epsilon_{\rm int}$ and $\epsilon_{\rm NP}$ for each leptoquark. The $n(Z/\gamma)$ and $n(\mathrm{SM})$ are, respectively, the number of Z/γ events and total number of SM events, expected by ATLAS (see Table 1).

Then we estimate a "confidence level" CL for the exclusion as follows. Consider first the case of constructive interference, where the SM + NP cross section is larger than the SM cross section. Then assuming Poisson statistics for the last three bins, the probability of counting the observed number N events or less, when expecting ν, is

$$P_b = e^{-\nu}\sum_{n\leq N}\frac{\nu^n}{n!}.$$

In the case of a leptoquark-mediated contact interaction with destructive interference, the expected number of SM + NP events in some bins is less than the expectation for the SM alone. For those bins, P_b is taken as the probability of observing more than or equal to the observed number N. The "confidence level" then is estimated as

$$\mathrm{CL}=1-\Pi_b\frac{P_b(\nu=\mathrm{SM}+\mathrm{NP})}{P_b(\nu=\mathrm{SM})} \tag{16}$$

These "confidence levels" are listed in the last column of Table 2, for the bounds quoted in the second last column [obtained from Eqs. (13) and (14)]. Our CL estimates are higher for the leptoquark limits than for the ATLAS contact

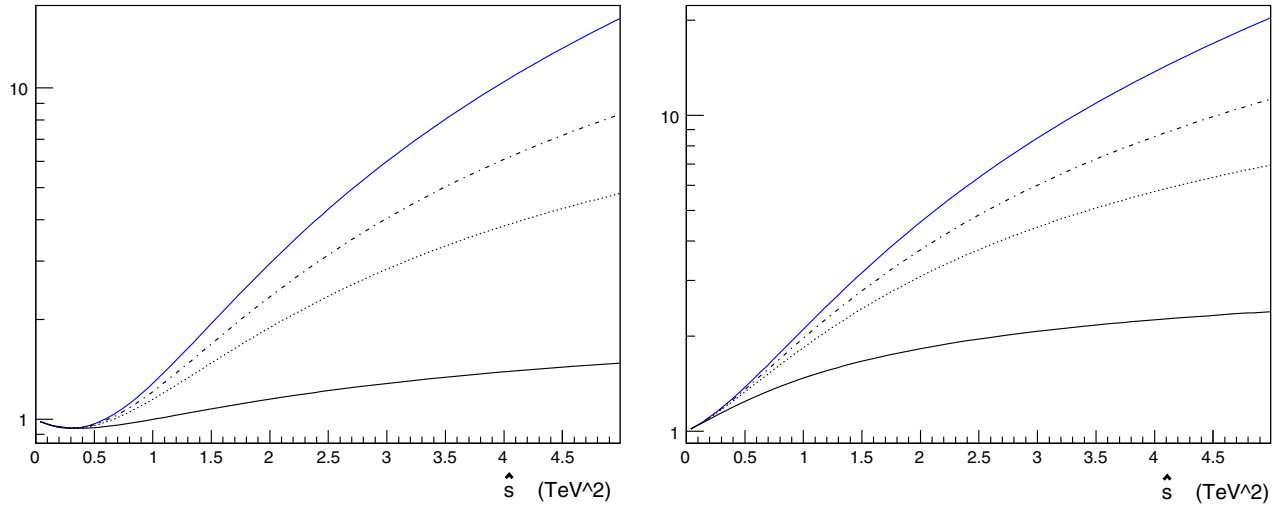

Fig. 3 Ratios of $d\sigma/d\hat{s}(Z/\gamma$ + New Physics) to $d\sigma/d\hat{s}(Z/\gamma)$—see Eqs. (11), (12) and (17). From the lowest curve upwards, the New Physics is a t-channel leptoquark with $m_{\rm LQ} = 1$ (*solid*), 2 (*dotted*) and 3 (*dash-dotted*) TeV, and finally a contact interaction with coefficient $\lambda^2/(2m^2) = 1/8$ TeV^{-2} (*blue*). The leptoquark couplings are chosen to reproduce the contact interaction in the $\hat{s} \to 0$ limit. On the *left*, destructive interference, constructive on the *right*

interaction, which reassures us that our bounds are conservative. However, the variation in the CLs indicates that Eq. (13) is not a reliable approximation. To obtain a consistent confidence level for various values of $\epsilon_{\rm int}/\sqrt{\epsilon_{\rm NP}}$ would require a more sophisticated study.

4 Including the leptoquark propagator

The aim of this section is to estimate the consequences of including the leptoquark propagator $1/(m_{\rm LQ}^2 - \hat{\tau})$ (where $\hat{\tau} \in \{\hat{t}, \hat{u}\}$, and recall $\hat{t}, \hat{u} < 0$), which only reduces to a contact interaction in the $|\hat{\tau}| \lesssim \hat{s} \ll m_{\rm LQ}^2$ limit. It is interesting to explore the $m_{\rm LQ}^2 \lesssim \hat{s}$ range, because the lower bound on the mass of pair-produced first generation leptoquarks is 830 GeV [4], whereas the highest bin in the ATLAS analysis is $\sqrt{\hat{s}} > 1800$ GeV.

The effect of the massive LQ propagator can be seen by comparing the partonic cross sections for LQ exchange versus a contact interaction. With the approximation of Eq. (10), $\mathrm{d}\sigma/\mathrm{d}\hat{s}$ for the ATLAS contact interaction is given in Eq. (12). In the same approximation, with the same values of $\epsilon_{\rm int} = 1/6$ and $\epsilon_{\rm NP} = 1$, $\mathrm{d}\sigma/\mathrm{d}\hat{s}$ for leptoquark exchange is

$$\frac{\mathrm{d}\sigma_{\rm LQ}}{\mathrm{d}\hat{s}} = \frac{\mathrm{d}\sigma_{Z/\gamma}}{\mathrm{d}\hat{s}} + \frac{C}{s\hat{s}}\left[\frac{g^2\lambda^2}{12}\left(\frac{1}{2} - \frac{m^2}{\hat{s}} + \frac{m^4}{\hat{s}^2}\ln\left(1+\frac{\hat{s}}{m^2}\right)\right) + \frac{\lambda^4}{4}\left(1 - 2\frac{m^2}{\hat{s}}\ln\left(1+\frac{\hat{s}}{m^2}\right) + \frac{m^2}{(m^2+\hat{s})}\right)\right]. \tag{17}$$

In Fig. 3 the differential cross sections for leptoquarks of masses 1, 2 and 3 TeV are plotted, and so is the contact interaction they induce (the leptoquark couplings are adjusted such that all three give the same contact interaction). It is clear that for $m_{\rm LQ}^2 > 4\hat{s}$, the contact interaction approximation reproduces leptoquark exchange to within 20 %. This is represented in Fig. 2 by the dotted vertical lines, to the right of which the contact interaction approximation should be justified.

To constrain a leptoquark of $m_{\rm LQ} \lesssim 3.6$ TeV using the ATLAS contact interaction analysis, we should account for the differences in the cross-section shape, as a function of $\hat{s}$. For the leptoquarks represented in Fig. 2, we estimate the value of λ which can be excluded for masses of 1, 2 and 3 TeV, by requiring that the estimated confidence level of the leptoquark exclusion, exceed the CL for the associated contact interaction. For instance, for S_2 with coupling λ_L, the bounds in the contact interaction (CI) approximation, including the propagator, are

$$\text{CI: } \lambda_L^2 < \begin{cases} 0.22, & m_{\rm LQ} = 1 \text{ TeV}, \\ 0.82, & m_{\rm LQ} = 2 \text{ TeV}, \\ 1.9, & m_{\rm LQ} = 3 \text{ TeV}, \end{cases}$$

$$\text{Propagator: } \lambda_L^2 < \begin{cases} 0.4, & m_{\rm LQ} = 1 \text{ TeV}, \\ 1.2, & m_{\rm LQ} = 2 \text{ TeV}, \\ 2.5, & m_{\rm LQ} = 3 \text{ TeV}. \end{cases} \tag{18}$$

The bounds obtained with the propagator are plotted as stars in Fig. 2. The bounds on S_2 are comparable [1] (weaker by ∼25 %) than those obtained in [10] by simulating leptoquark exchange in Madgraph and compared to "large extra dimension" searches in 20 fb^{-1} of data. As expected, the effect of

[1] It was unclear to the authors which leptoquark couplings were simulated, with which interference.

the leptoquark mass, for $m_{\rm LQ}^2 \lesssim \hat{s}$ is to weaken the bound. The behaviour is straightforward for constructive interference, however, for destructive interference, the CL of Eq. (16) does not increase monotonically with coupling, at fixed mass: increasing the coupling redistributes the excesses and deficits among bins, so cancellations can allow a larger coupling to be less excluded than a smaller one. We do not pursue this issue, because it depends sensitively on the binning.

5 Discussion

A signal for a contact interaction of coefficient λ^2/m^2 is a plateau at the high-energy end of a decreasing distribution, possibly preceded by a valley in the case of destructive interference with the SM. For $q\bar{q} \to e^+e^-$, the exchange of Z/γ is the principal SM contribution, responsible for the cross section decreasing as $1/\hat{s}$. So one expects a sensitivity to

$$\frac{\lambda^2}{m_{\rm LQ}^2} \gtrsim \frac{g^2}{M^2_{e^+e^-,\max}} \tag{19}$$

where $M^2_{e^+e^-,\max}$ is the e^+e^- invariant mass-squared of the highest bin. The contact interaction approximation is expected to be valid for $m_{\rm LQ}^2 \gg \hat{s}$, and λ^2 below a strong coupling/unitarity bound:

$$\lambda^2 \lesssim 4\pi, \quad m_{\rm LQ}^2 > 4M^2_{e^+e^-,\max} \tag{20}$$

where the inequality representing the $\hat{s} \ll m_{\rm LQ}^2$ bound is chosen from Fig. 3. This gives a triangular region in $\lambda, m_{\rm LQ}$ parameter space (above the diagonal, and to the right of the dotted line in Fig. 2), where contact interaction searches at colliders are well defined. Nonetheless there should also be a reduced sensitivity to the exchange of less-heavy off-shell particles with $m^2 \sim \hat{s}$.

The aim of this paper was twofold. First, our aim was to extract bounds on leptoquarks from the LHC searches for contact interactions in the process $pp \to e^+e^- + X$. Leptoquarks interacting with electrons and first generation quarks could contribute to $q\bar{q} \to e^+e^-$ via t-channel exchange. In Table 2 are quoted the limits laboriously obtained from an ATLAS analysis [5], using the contact interaction approximation and some hopefully conservative analytic arguments (see also Table 3 of the "note added"). The limits have varying confidence levels, indicating the difficulty of translating current bounds to leptoquarks. Including the leptoquark propagator can modify these bounds. For leptoquark masses $\gtrsim$ TeV and constructive interference between the leptoquark and the SM, the propagator weakens the bound on λ^2 by less than a factor 2 [see Eq. (18) and Fig. 3]. The case of destructive interference is more delicate; if a model predicts deficits and excesses with respect to SM expectations in various $\hat{s}$ ranges, whether these may cancel in the data will depend on the binning. Indeed, it is common to neglect the deficits predicted in models with destructive interference, and set bounds by requiring that they not produce excesses [7,10].

Table 3 Upper bounds on λ^2 for various scalar leptoquarks interacting with first generation leptons and quarks. The leptoquark and coupling are given in the left column [notation of Eq. (4)], and the mass is given in the top row. These bounds are obtained by combining the formulae of this paper for $\epsilon_{\rm int}, \epsilon_{\rm NP}$, with [8] where recent CMS data [7] was fit to a parametrisation of the cross section. These bounds are based on more data than those of Table 2, so they are more stringent

Leptoquark	$m_{\rm LQ}=3$ TeV, $\lambda^2 <$	$m_{\rm LQ}=2$ TeV, $\lambda^2 <$	$m_{\rm LQ}=1$ TeV, $\lambda^2 <$
S_o, λ_{LS_o}	0.54	0.24	0.07
S_o, λ_{RS_o}	0.54	0.24	0.07
$\tilde{S}_o, \lambda_{R\tilde{S}_o}$	1.4	0.74	0.32
S_2, λ_L	0.90	0.48	0.20
S_2, λ_R	0.84	0.45	0.20
$\tilde{S}_2, \lambda_{L\tilde{S}_2}$	1.9	0.98	0.47
S_1, λ_{LS_1}	0.94	0.49	0.23

The second aim of this paper was to explore whether experimental bounds on a selection of contact interactions can be readily translated to New Physics scenarios. The answer is no. There are two issues which arise:

1. Many of the channels in which contact interactions are searched for (for instance $qq \to qq$, or $q\bar{q} \to e^+e^-$) can be mediated by the SM. So the SM + NP cross section is of the form $|\text{SM}|^2$ + interference + $|\text{NP}|^2$, as given in Eq. (9). The sign and magnitude of the interference term (relative to $|\text{NP}|^2$) depend on the flavours and chiralities of the contact interaction, and cause the number of events to increase or decrease. In general, experimental bounds are quoted only for a few magnitudes of the interference term, so they cannot be applied to the majority of models (as in the case here, none of the leptoquarks induce the contact interaction studied by ATLAS). It is not sufficient for the experimental collaborations to set bounds on a complete set of contact interactions, because a model can induce a linear combination of contact interactions, and there is no way to make a linear combination of bounds. An alternative, presented in [6] and pursued in [8], is to set simultaneous bounds on the coefficients of the $|\text{NP}|^2$ and interference terms in the cross section. This approach is followed in the "note added".
2. The four-momentum of the new particle mediating the "contact interaction" can only be neglected if the new particle is very heavy and strongly coupled. If the propagator $\sim 1/(\hat{t}-m^2)$ of a new particle exchanged in the t-channel is retained, the contact interaction is suppressed, because $\hat{t} \sim -\hat{s}$. In the case of leptoquarks, we estimated here that this weakens the bounds on λ^2 by a factor of order

2 [see Eq. (18)]. Also this problem can be addressed by fitting data to the form of the cross section, as performed in [8].

In summary, we estimated that ATLAS contact interaction searches in $pp \to e^+e^-$ at the 7 TeV LHC can exclude first generation leptoquarks with couplings $\lambda^2 \gtrsim m_{\rm LQ}^2/(2\ {\rm TeV})^2$ (see Table 2 for specific bounds). Two difficulties arose in translating the experimental bounds to all the possible leptoquarks. The most significant problem is that the sign and size of the interference with the SM varies from one leptoquark to another, and it significantly affects the shape of the cross section and therefore the bounds. Secondly, the leptoquarks are rarely heavy enough to justify neglecting their four-momentum in the propagator, which, when included, can weaken the bound on λ^2 by $\sim$50 %. These problems could be addressed by fitting the data to a form factor parametrisation of the cross section, as discussed in [6,8]. This is pursued in the "note-added", using more recent and restrictive data, and gives the bounds in Table 3.

Note added

The CMS Collaboration recently presented [7] contact interaction bounds obtained from 20 fb^{-1} of 8 TeV $q\bar{q} \to \ell^+\ell^-$ data ($\ell = e, \mu$). In [8], one of the authors and other collaborators attempted to fit the plots of [7] to a "form factor" parametrisation of the cross section:

$$\frac{{\rm d}\sigma}{{\rm d}\hat{s}} = \frac{{\rm d}\sigma_{DY}}{{\rm d}\hat{s}}\left(1 + a\frac{\hat{s}}{1+c\hat{s}} + b\frac{\hat{s}^2}{(1+c\hat{s})^2}\right). \tag{21}$$

Allowed ellipses in a, b space were obtained for different values of the leptoquark mass-squared $1/c$. The a, b parameters are simply related to $\lambda^2/m_{\rm LQ}^2$, $\epsilon_{\rm int}$ and $\epsilon_{\rm NP}$ of Table 2, so bounds on λ^2 for $m_{\rm LQ} = 1, 2, 3$ TeV can be read from the plots of [8] and are given in Table 3. The larger CMS dataset gives more restrictive bounds than the earlier ATLAS publication. The 95 % C.L. bounds of Table 3 are more reliable than those estimated in Table 2, and they are easily obtained from the ellipses of [8]. In our opinion, the experimental bounds from the high-energy tails of distributions would be easier to apply to heavy new particles if the data was parametrised as suggested in [6,8].

Acknowledgments We thank Sébastien Descotes-Genon for checks and comments.

References

1. J. Beringer et al., Particle Data Group, Phys. Rev. D **86**, 010001 (2012)
2. S. Davidson, D.C. Bailey, B.A. Campbell, Model independent constraints on leptoquarks from rare processes. Z. Phys. C **61**, 613 (1994). arXiv:hep-ph/9309310
3. J.L. Hewett, T.G. Rizzo, Much ado about leptoquarks: a comprehensive analysis. Phys. Rev. D **56**, 5709 (1997). arXiv:hep-ph/9703337
4. S. Chatrchyan et al., CMS Collaboration, Search for pair production of first- and second-generation scalar leptoquarks in pp collisions at $\sqrt{s} = 7$ TeV. Phys. Rev. D **86**, 052013 (2012). arXiv:1207.5406 [hep-ex]
5. G. Aad et al., ATLAS Collaboration, Search for contact interactions and large extra dimensions in dilepton events from pp collisions at $\sqrt{s} = 7$ TeV with the ATLAS detector. Phys. Rev. D **87**, 015010 (2013). arXiv:1211.1150 [hep-ex]
6. J. de Blas, M. Chala, J. Santiago, Global constraints on Lepton–Quark contact interactions. Phys. Rev. D **88**, 095011 (2013). arXiv:1307.5068 [hep-ph]
7. The CMS Collaboration, Search for contact interactions in Dilepton mass spectra in pp collisions at $\sqrt{s} = 8$ TeV, CMS-PAS-EXO-12-020
8. S. Davidson, S. Descotes-Genon, P. Verdier, Of contact interactions and colliders, arXiv:1410.4798 [hep-ph]
9. H. Pirumov, QCD analysis of neutral and charged current cross sections and search for contact interactions at HERA, DESY-THESIS-2013-051
10. M.B. Wise, Y. Zhang, Effective theory and simple completions for neutrino interactions. Phys. Rev. D **90**, 053005 (2014). arXiv:1404.4663 [hep-ph]
11. H. An, X. Ji, L.T. Wang, Light dark matter and Z' dark force at colliders. JHEP **1207**, 182 (2012). arXiv:1202.2894 [hep-ph]
12. G.D. La Rochelle, M. Elmer, Heavy Z': resonant versus non-resonant searches. arXiv:1406.2547 [hep-ph]
13. I. Dorsner, S. Fajfer, A. Greljo, Cornering scalar leptoquarks at LHC. JHEP **1410**, 154 (2014). arXiv:1406.4831 [hep-ph]
14. W. Buchmuller, R. Ruckl, D. Wyler, Leptoquarks in lepton quark collisions. Phys. Lett. B **191**, 442 (1987); Erratum-ibid. B **448**, 320 (1999)
15. T. Sjostrand, S. Mrenna, P.Z. Skands, PYTHIA 6.4 physics and manual. JHEP **0605**, 026 (2006). arXiv:hep-ph/0603175